J. Innovative Eng. Nat. Sci., vol. 5, no. 2, pp. 751-764, 2025.
http://doi.org/10.61112/jiens.1666125

Original Paper

Journal of Innovative Engineering and Natural Science

(Yenilikçi Mühendislik ve Doğa Bilimleri Dergisi)

https://dergipark.org.tr/en/pub/jiens

Influence of shear wall layout on the seismic performance of an RC building

Aytug Seckin[a]*

[a]*Kocaeli University, Department of Civil Engineering, Kocaeli 41001, Türkiye.*

ARTICLE INFO

Article history:
Received 26 March 2025
Received in revised form 23 May 2025
Accepted 18 June 2025

Available online

Keywords:
Reinforced concrete buildings
Shear wall layout
Nonlinear time-history analysis
Seismic performance evaluation
Turkish Building Earthquake Code

ABSTRACT

The seismic behavior of shear walls plays a crucial role in the overall structural response by enhancing lateral stiffness, strength, and energy dissipation capacity. This study investigates the influence of shear wall layout on the seismic performance of a 10-story reinforced concrete (RC) building. For this purpose, three models with perimeter shear walls, shear walls along the middle axes, and a core shear wall are designed in accordance with the Turkish Building Earthquake Code (TBEC-2018). Nonlinear time-history analyses are conducted on these models using two approaches: (i) scaled ground motion records matching the design spectrum (Case-1) and (ii) the unscaled ground motion record from the Pazarcık (Kahramanmaraş) earthquake (Case-2). While all models satisfy the Controlled Damage (CD) performance level under Case-1, only the model with a core shear wall remains within this performance level under Case-2. Additionally, the models are assessed in terms of base shear, hysteretic energy dissipation, and top-story displacement demands. The study reveals that the model with a core shear wall exhibits better seismic performance than the other layouts, particularly under the Pazarcık (Kahramanmaraş) earthquake.

I. INTRODUCTION

Reinforced concrete (RC) shear walls are widely used vertical structural elements in earthquake-resistant building design. When appropriately placed within the floor plan, shear walls reduce non-structural damage during moderate earthquakes and enable controlled plastic hinge formation in designated regions under severe seismic effects, thereby preventing total collapse. As the number of stories increases, the incorporation of shear walls becomes essential for achieving an efficient and cost-effective design and limiting excessive inter-story drifts that could lead to severe structural damage [1]. In this context, it is important to examine the influence of shear wall layout on the seismic performance of RC buildings.

Most studies in the literature on shear wall layout have focused on evaluating its effect on inter-story drift, lateral displacement, base shear, and/or internal force demands in buildings using linear analysis methods [2-13]. Aminnia and Hosseini [14] investigated the influence of shear wall placement and cross-sectional shape on the seismic responses of multi-story RC buildings with plan irregularities. They conducted nonlinear time-history analyses on buildings with different shear wall configurations, including rectangular, L-, T-, U-, and Z-shaped walls, positioned either at the core or along the perimeter frames. Their findings indicated that U-shaped shear walls placed at the central core and Z-shaped walls located at the corners exhibited better seismic performance. Resatoglu and Jkhsi [15] investigated the effects of shear wall position and thickness on the ductility of two-dimensional RC dual systems using pushover analysis, concluding that relocating shear walls from the perimeter to the middle of the frame caused a reduction in ductility. Khelaifia et al. [16] examined the impact of shear wall position and shear

*Corresponding author. Tel.: +90-262-303-3271; e-mail: aytug.seckin@kocaeli.edu.tr

wall-to-floor area ratio on the seismic performance of an eight-story RC building through pushover analysis. Their study revealed that placing shear walls in the middle of the structure, instead of along the periphery, resulted in better performance, and shear walls with compound configurations (e.g., box, U, L) enhanced structural reliability in terms of inter-story drift. Labibzadeh et al. [17] examined the effect of shear wall placement on the seismic fragility curves of regular and irregular two-dimensional RC frames subjected to sequential earthquake excitations. Beyond planar layout effects, studies by Sesli et al. [18, 19] have examined the behavior of RC coupled shear wall systems under cyclic loading, with particular focus on coupling beam types and wall boundary detailing. One study [18] investigated systems with conventionally and diagonally reinforced coupling beams, while another [19] extended the scope to include steel coupling beams. These studies highlight the influence of coupling beam design and wall boundary detailing on ductility, hysteretic behavior, stiffness degradation and energy dissipation capacity, which collectively contribute to the overall seismic performance of RC coupled shear wall systems. These parameters may be regarded as complementary components to the enhanced structural response provided by optimal shear wall layout.

In this study, three structural models are developed to assess the influence of shear wall layout on the seismic performance of a 10-story RC building. The layouts investigated include perimeter shear walls, shear walls along the middle axes and a core shear wall. The models are designed in accordance with the provisions of the Turkish Building Earthquake Code (TBEC-2018) [20]. To contribute to the limited number of studies examining this influence through nonlinear methods, nonlinear time-history analyses (NLTHAs) are conducted on these models. The compliance of these models with the prescribed performance targets is evaluated. In this context, three key structural response parameters are examined: base shear, hysteretic energy dissipation and top-story displacement. The findings reveal that the model with a core shear wall exhibits better seismic performance than the other layouts.

II. DESIGN OF THE MODELS ACCORDING TO TBEC-2018

To investigate the influence of shear wall layout on the seismic performance of a building, three models are developed. These models are labeled as Model-1, Model-2 and Model-3, corresponding to shear walls located at the perimeter, along the middle axes and in the core, respectively. The models have a symmetrical structural layout in plan, with each floor measuring 22×22 meters. Designed for residential use, the 10-story models incorporate high-ductility reinforced concrete frames and shear walls as their lateral load-resisting system (Figure 1). The fundamental periods of the models are 1.08 s, 1.06 s, and 0.81 s for Model-1, Model-2, and Model-3, respectively.

The design of the models is conducted using response spectrum analysis in accordance with the provisions of TBEC-2018. The horizontal elastic design spectrum, corresponding to the standard earthquake ground motion level (DD-2) with a 10% probability of exceedance in 50 years, is generated using the seismic hazard map of Türkiye, developed by the Disaster and Emergency Management Presidency (AFAD) [21], considering local soil class ZC. Structural analyses are performed using SAP2000 v23 software [22]. Beams and columns are modeled with frame elements, while shear walls and slabs are modeled with area elements. The rigid diaphragm assumption is adopted for slabs. Effective stiffness coefficients are applied to model the cross-sectional properties of the structural elements. The response modification coefficient (R) and overstrength factor (D) are taken as 7 and 2.5, respectively. The models are assigned an importance factor (I) of 1 based on their intended use and are classified in seismic design category 1, in accordance with the short-period design spectral acceleration coefficient.

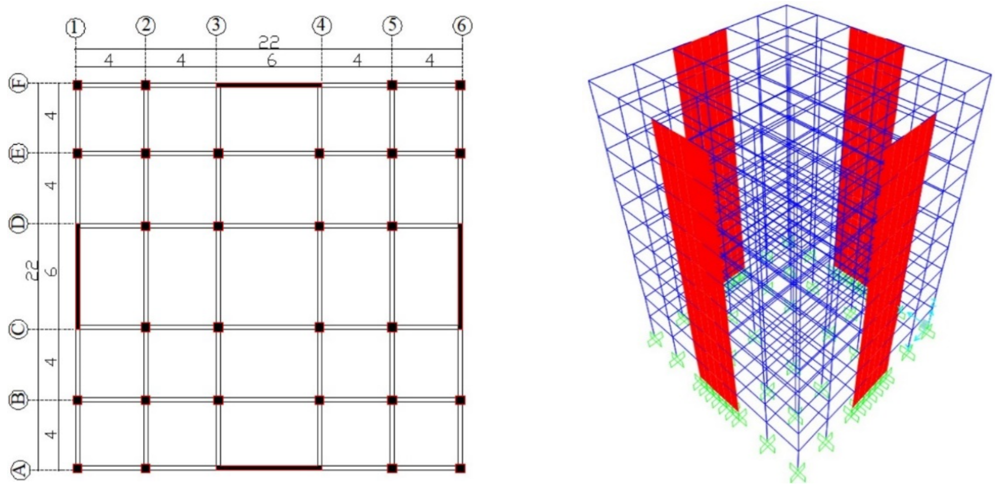

(a)

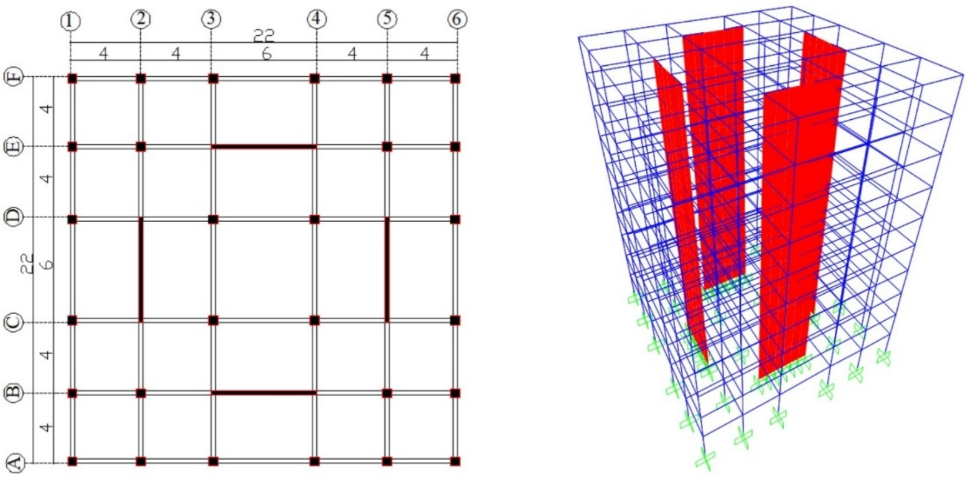

(b)

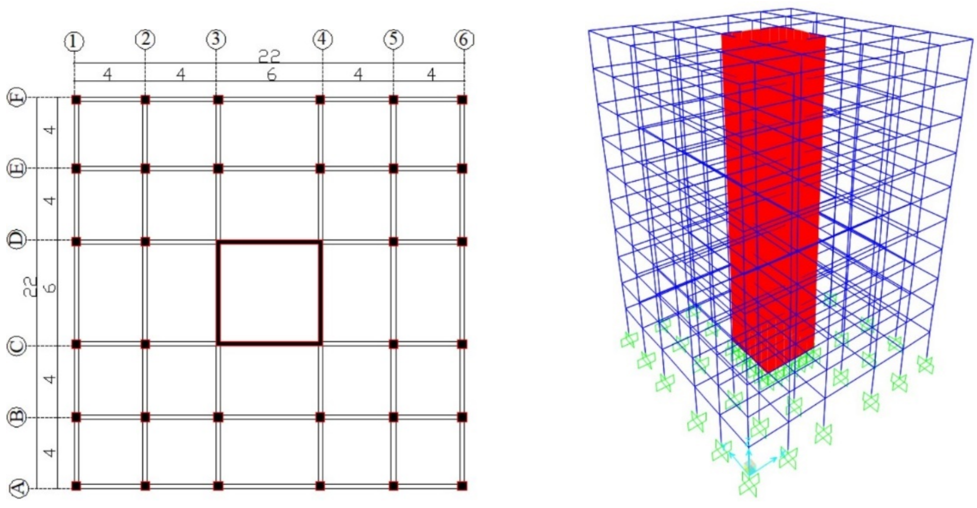

(c)

Figure 1. Structural systems and numerical models **(a)** Model-1 **(b)** Model-2 **(c)** Model-3 (All lengths are in meters)

All models are designed with identical material properties and structural element dimensions for comparison. Concrete class C30 is selected, while B420C steel is used for both longitudinal and transverse reinforcement.

Cross-sectional dimensions are 0.50×0.50 m for columns and 0.25×0.50 m for beams, while the slab thickness is 0.15 m for all stories. Rectangular shear walls are designed with a length of 6 meters in plan and a thickness of 0.25 meters. The shear wall length is determined based on the overturning moment demands at the base under seismic loads, as well as the inter-story drift limit requirements. As a result of the design process, the minimum longitudinal reinforcement ratios specified in TBEC-2018 are found to be sufficient for RC columns and shear walls (Figure 2).

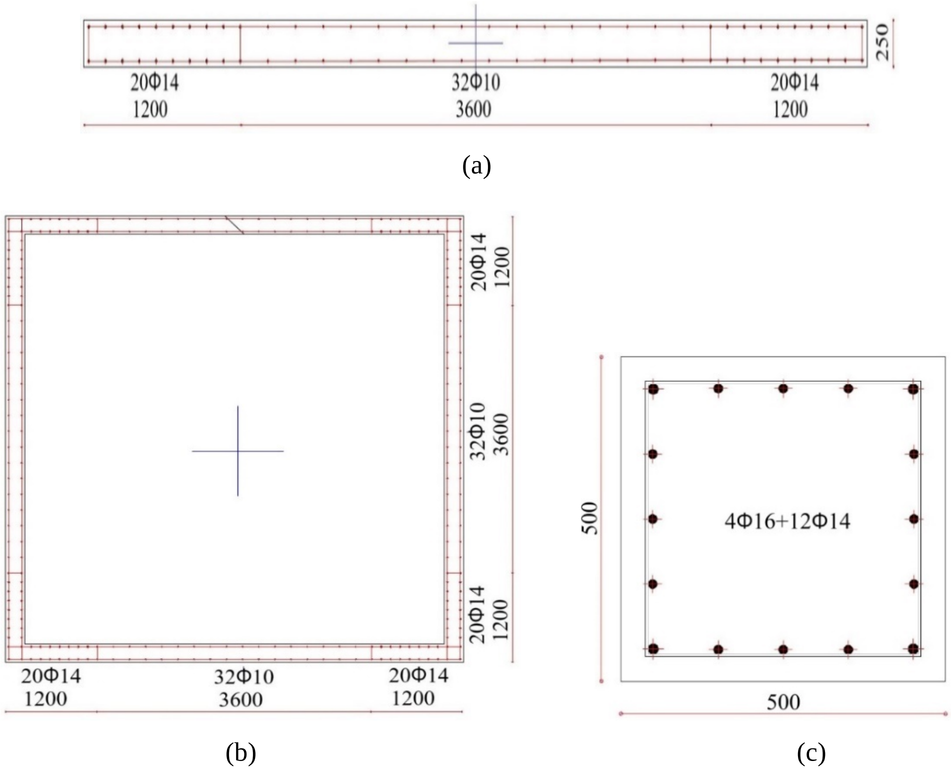

Figure 2. Cross-section details of **(a)** first-story shear walls in Model-1 and Model-2 **(b)** first-story core shear wall in Model-3 **(c)** typical columns (All dimensions are in millimeters)

Table 1 presents the fundamental periods and the corresponding mass participation ratios in the X (UX) and Y (UY) directions for each model.

Table 1. Fundamental periods and corresponding mass participation ratios

Model	**Period** (s)	**UX**	**UY**
Model-1	1.08	0.0001	0.7147
Model-2	1.06	0.0106	0.7076
Model-3	0.81	0.0004	0.7055

III. NONLINEAR ANALYSES

According to TBEC-2018, the assessment of existing buildings shall be conducted using the Deformation-Based Assessment and Design (DBD) approach. Nonlinear pushover and time-history analyses can be conducted within the DBD framework. In this study, nonlinear time-history analyses (NLTHAs) are performed. The nonlinear behavior is captured by assigning M3 plastic hinges at the ends of beam elements to represent bending behavior. For column elements, fiber hinges with P–M2–M3 interaction are used to capture the combined effects of axial load and bending. In the fiber element model, the concrete is discretized into sufficiently small cells, while the reinforcing bars are represented as separate elements. Nonlinear axial stress-strain relationships for both concrete and reinforcing bars are considered in each cell (Figure 3a). Figure 3(b) presents the moment–rotation hysteresis curve at the base of a first-story column during the Pazarcık (Kahramanmaraş) earthquake. The hysteretic response reflects the nonlinear hinge behavior defined by Ibarra et al. [23], exhibiting strength and stiffness degradation, along with notable energy dissipation. The nonlinear behavior of shear walls is represented using a multi-layered shell element model based on composite material mechanics. This model captures nonlinear in-plane and out-of-plane bending behavior, as well as in-plane shear behavior. The shell element can be composed of multiple layers with varying thicknesses and material properties. Within the framework of the finite element method, the axial strain and curvature of the middle layer are first computed. Given the validity of the plane section assumption, the strains and curvatures of the remaining layers are derived accordingly. The corresponding stresses are then calculated using the constitutive models of the materials assigned to each layer [24-25] (Figure 3c).

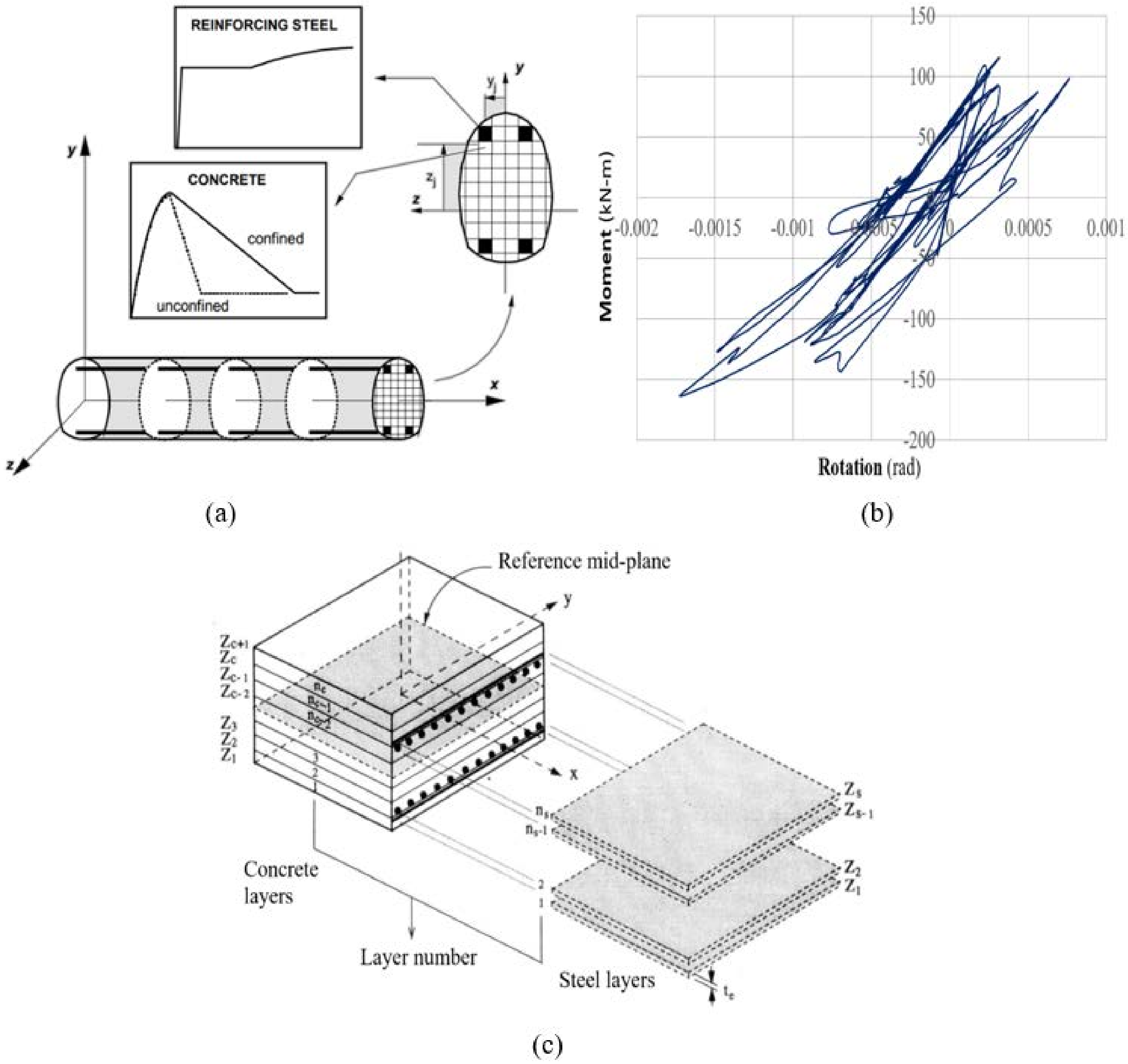

Figure 3. (a) Fiber element model [26] **(b)** Moment–rotation hysteresis curve of a first-story column **(c)** Multi-layered shell element model [27]

The Mander model [28] is used to represent confined and unconfined concrete behavior, while the stress–strain relationship of reinforcing steel is defined based on the constitutive equations specified in TBEC-2018. The initial condition for NLTHA is established by performing an incremental static analysis under vertical loads. Seismic analysis is performed by simultaneously applying horizontal acceleration components along two orthogonal directions of the structural system. The Newmark integration method and Rayleigh damping model are employed in the analyses. The Rayleigh damping coefficients are determined by assigning a 5% damping ratio at two selected vibration periods: one corresponding to the fundamental mode and the other to a higher mode in which the cumulative mass participation exceeds 90%.

Two cases are defined for the ground motion records applied to the building. In the first case (Case-1), NLTHAs are performed using a set of three scaled ground motion records in accordance with Eurocode-8 [29]. Eurocode 8 requires the use of at least three accelerograms, and if only three are used, the most unfavorable response shall be considered. Acceleration records are selected based on a moment magnitude (M_w) greater than 6.5 and a Joyner–Boore distance (R_{jb}) less than 20 km [30]. The records are obtained from the Pacific Earthquake Engineering Research Center (PEER) [31] database. The characteristics of the selected acceleration records are presented in Table 2.

Table 2. Ground motion records used in Case-1 (M_w: Moment magnitude; R_{jb}: Joyner–Boore distance)

Ground Motion	Station	Components	M_w	R_{jb} (km)	Scale Factor
Chi-Chi, Taiwan	TCU129	E, N	7.62	1.83	0.70
Niigata, Japan	NIGH11	EW, NS	6.63	6.27	0.91
Darfield, New Zealand	DSLC	27, 63	7.00	5.28	1.34

The average response spectrum of the selected ground motion records is scaled so that it does not fall below the design spectrum ordinates within the period range from 0.2 times the shortest fundamental period (Model-3, 0.81 s) to 1.5 times the longest fundamental period (Model-1, 1.08 s). This period range is selected to adequately capture the dynamic characteristics of all three structural models. The scaled average response spectrum and 1.3 times the ordinates of the elastic design spectrum are presented in Figure 4(a), where T_p denotes the fundamental period of the structure.

On February 6, 2023, devastating earthquakes (M_w=7.7 and M_w=7.6) centered in Kahramanmaraş, Türkiye, caused numerous buildings across 11 provinces to collapse or suffer severe damage, resulting in significant loss of life. In the second case (Case-2), NLTHAs are conducted using the ground motion data recorded at Station 4625 during the Pazarcık (Kahramanmaraş) earthquake. The objective of this paper is to evaluate the structural response of the models to this specific seismic excitation. The ground motion record is obtained from the Turkish Accelerometric Database and Analysis System (TADAS) [32], and its characteristics are provided in Table 3. Figure 4(b) presents the response spectrum of this ground motion, the horizontal elastic design spectrum, and the acceleration spectrum corresponding to the DD-1 earthquake level (2% probability of exceedance in 50 years).

Table 3. Ground motion record used in Case-2 (M_w: Moment magnitude; ED: Epicentral distance)

Ground Motion	Station	Components	M_w	ED (km)
Pazarcık (Kahramanmaraş)	4625	E, N	7.70	28.40

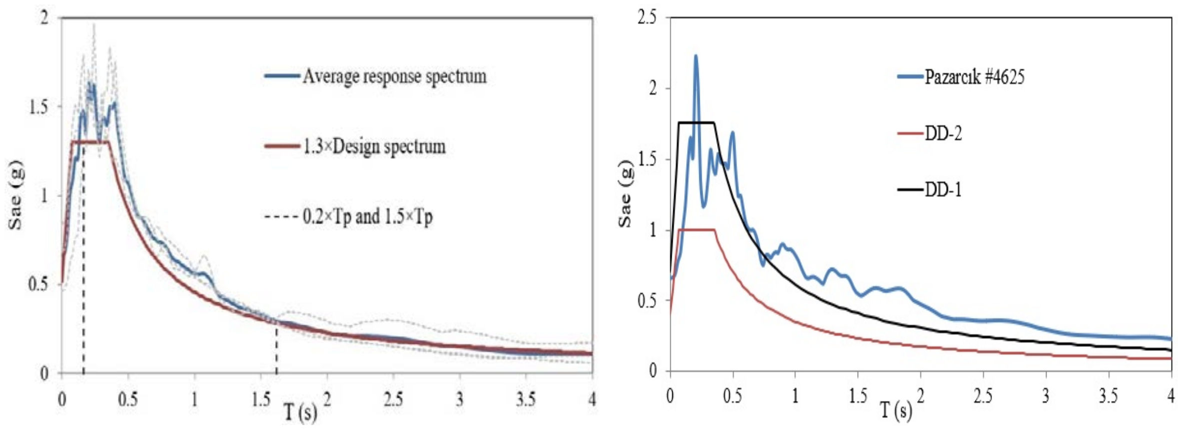

(a) (b)

Figure 4. (a) Scaled average response spectrum of the ground motion records in Case-1 **(b)** Response spectrum of the Pazarcık earthquake record in Case-2

IV. RESULTS AND DISCUSSION

In TBEC-2018, three damage states and their corresponding limits are defined at the cross-sectional level to describe inelastic behavior: Limited Damage (LD), Controlled Damage (CD), and Collapse Prevention (CP). In addition, four damaged regions are specified: Limited Damage, Significant Damage, Extreme Damage, and Collapse (Figure 5).

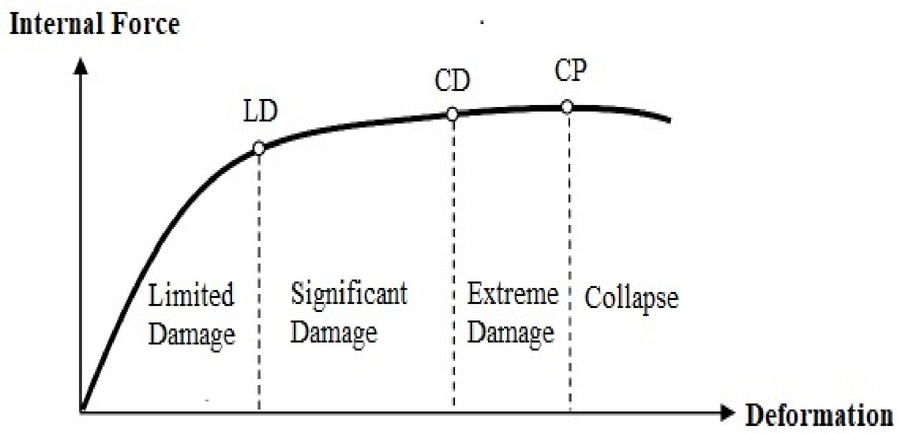

Figure 5. Damage states and regions according to TBEC-2018

4.1 Performance Evaluation for Case-1

According to TBEC-2018, the performance target for existing buildings classified as seismic design category 1 is the Controlled Damage (CD) performance level under DD-2 ground motion. Buildings that meet the following criteria are at this performance level:

a. In each story, no more than 35% of the beams and a specified portion of the vertical elements may reach the extreme damage region.

b. All other structural elements shall remain within the limited damage or significant damage regions.

The analysis results for Case-1 indicate that all models satisfy the Controlled Damage (CD) performance level. The maximum reinforcement strains ($\varepsilon_{s,max}$) at the base of the first-story columns of Model-1, Model-2, and Model-3 are 0.0027, 0.0020 and 0.0014, respectively. The corresponding maximum concrete compressive strains ($\varepsilon_{c,max}$) are -0.0015, -0.0011 and -0.0010. For the first-story shear walls, the maximum reinforcement strains ($\varepsilon_{s,max}$) are 0.0118, 0.0088 and 0.0118, while the maximum concrete compressive strains ($\varepsilon_{c,max}$) are -0.0025, -0.0023 and -0.0016 for Model-1, Model-2, and Model-3, respectively. The maximum plastic hinge rotations of beams are 0.0139, 0.0125 and 0.0134 for the respective models. Based on these results, all structural elements in the models remain within the CD limit.

Seckin and Doran [33] stated that the Modified Modal Superposition (MMS) approach [34] enables a design that satisfies the shear capacity requirements in RC walls. The maximum shear demands at the base of the shear walls are calculated as 3918 kN, 3937 kN, and 7271 kN for Model-1, Model-2, and Model-3, respectively. Using the MMS approach, the base shear forces for Model-1, Model-2, and Model-3 are computed as 4664 kN, 4676 kN, and 9480 kN, respectively. These results confirm that the MMS approach ensures shear safety in RC walls.

Figure 6 presents the time histories of base shear for the models. The maximum base shear values are 9794 kN, 10394 kN, and 13290 kN for Model-1, Model-2, and Model-3, respectively. Among the three models, Model-3 exhibits the highest base shear demand.

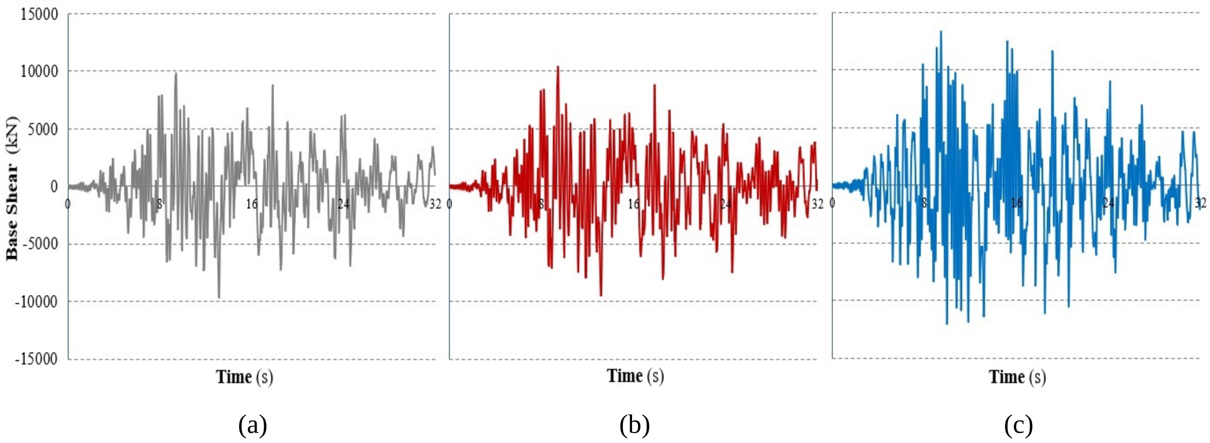

Figure 6. Time history of base shear under Case-1 **(a)** Model-1 **(b)** Model-2 **(c)** Model-3

Figure 7 presents the total hysteretic energy dissipation of shear walls in each model, with values of 304.6 kN·m, 229.5 kN·m, and 486.5 kN·m for Model-1, Model-2, and Model-3, respectively. Among the three models, Model-3 exhibits the highest energy dissipation, while Model-2 exhibits the lowest.

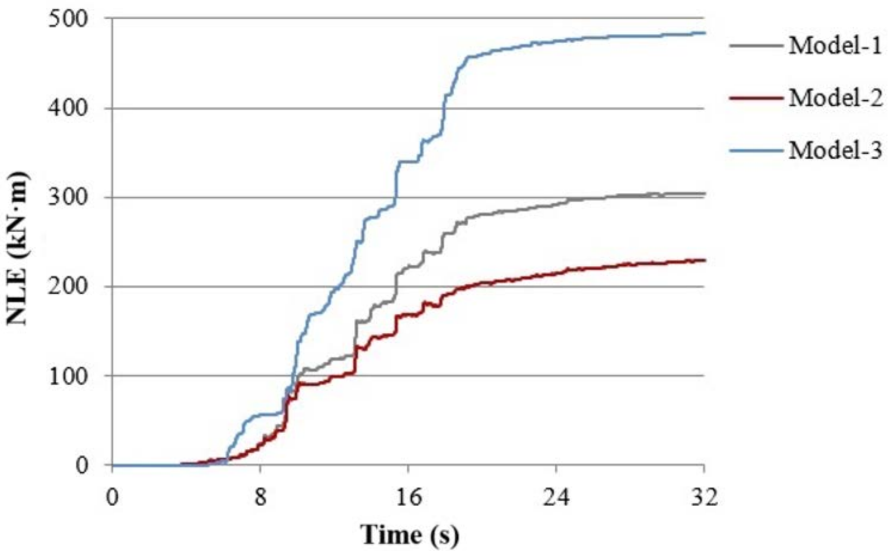

Figure 7. Total hysteretic energy dissipation of shear walls under Case-1 **(a)** Model-1 **(b)** Model-2 **(c)** Model-3

4.2 Performance Evaluation for Case-2

The fundamental objective of earthquake-resistant design is to ensure life safety during severe earthquakes by limiting permanent structural damage. In Case-2, the Pazarcık (Kahramanmaraş) earthquake is selected to evaluate the seismic response of the models under such severe ground motion. The analysis considers the strong-motion phase of the Pazarcık earthquake, which lasts for 20 seconds. Figure 8 shows the distribution of plastic hinges in the models, based on the envelope of all time steps obtained from NLTHAs.

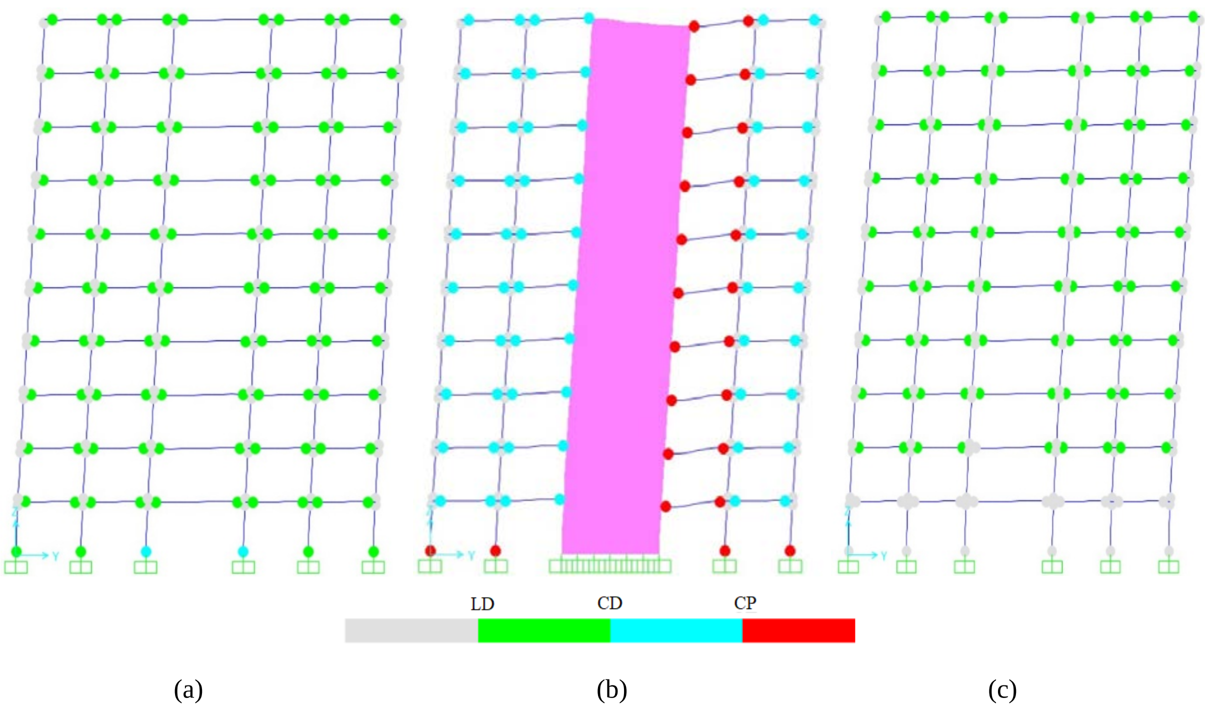

Figure 8. Distribution of plastic hinges under Case-2 **(a)** Model-1 **(b)** Model-2 **(c)** Model-3

A building is considered to satisfy the Collapse Prevention (CP) performance level if the following conditions are met:

a. In RC buildings, no more than 20% of the beams in any story may reach the collapse region.
b. All other structural elements shall remain within the limited, significant, or extreme damage regions.

Table 4 presents the damage regions of the first-story columns for each model. In Model-1, 57% of the columns remain within the CD limit, while the remaining 43% fall within the region of extreme damage. Model-2 exhibits the most severe response, with 96% of the columns exceeding the CP limit and only 4% falling within the extreme damage region. In contrast, Model-3 demonstrates the best performance, as all columns remain within the CD limit, with none of them reaching extreme damage or collapse regions.

Table 4. Damage regions of the first-story columns

Model	**Limited/Significant Damage** (%)	**Extreme Damage** (%)	**Collapse** (%)
Model-1	57	43	-
Model-2	-	4	96
Model-3	100	-	-

Table 5 provides an overview of the damage distribution in beams. In Model-1, the majority of beams remain within the CD limit (89–93%), with 7–11% reaching the extreme damage region. Model-2 exhibits a more severe response, with 36–43% of the beams within the CD limit, 50–60% within the extreme damage region, and up to 7% exceeding the CP limit. In contrast, Model-3 demonstrates the best performance, with nearly all beams (96–100%) remaining within the CD limit and only 4% reaching the extreme damage region.

Table 5. Damage regions for RC beams

	Model 1		**Model 2**			**Model 3**	
Story	**Limited/ Significant Damage** (%)	**Extreme Damage** (%)	**Limited/ Significant Damage** (%)	**Extreme Damage** (%)	**Collapse** (%)	**Limited/ Significant Damage** (%)	**Extreme Damage** (%)
1	93	7	36	59	5	100	0
2	91	9	36	59	5	96	4
3	89	11	36	59	5	96	4
4	89	11	36	59	5	96	4
5	89	11	36	59	5	96	4
6	89	11	36	59	5	96	4
7	89	11	36	60	4	96	4
8	89	11	43	50	7	96	4
9	89	11	43	50	7	96	4
10	89	11	43	50	7	96	4

Table 6 presents the damage regions of the first-story shear walls for the three models, with a detailed evaluation provided below.

Model-1:

- In shear walls SW-1 and SW-2, the reinforcement strain ($\varepsilon_s = 0.040$) exceeds the CP limit ($\varepsilon_s^{(CP)} = 0.032$), placing them in the collapse region.
- Additionally, the concrete compressive strain ($\varepsilon_c = -0.028$) in these walls is twice the CP limit ($\varepsilon_c^{(CP)} = -0.014$).
- The other shear walls (SW-3 and SW-4) remain within the significant damage region.

Model-2:

- The reinforcement strain ($\varepsilon_s = 0.031$) in shear walls SW-1 and SW-2 exceed the CD limit ($\varepsilon_s^{(CD)} = 0.024$).
- More critically, the concrete compressive strain ($\varepsilon_c = -0.116$) in these walls far exceeds the CP limit ($\varepsilon_c^{(CP)} = -0.014$). This excessive strain indicates severe crushing of the concrete, leading to a complete loss of load-bearing capacity.
- The other shear walls (SW-3 and SW-4) remain within the significant damage region.

Model-3:

- The reinforcement strain ($\varepsilon_s = 0.023$) in the shear walls is close to the CD limit ($\varepsilon_s^{(CD)} = 0.024$); however, all sections remain within the significant damage region.
- The maximum shear demand at the base of the shear wall is 8321 kN, which is safely met by the MMS approach, demonstrating its reliability in ensuring shear safety.

This evaluation highlights that Model-3 exhibits the best structural response, as all shear walls remain within the significant damage region, whereas those in Model-1 and Model-2 exceed the CP limit.

Table 6. Damage regions of the first-story shear walls

	Shear Wall	$\varepsilon_{c,max}$	$\varepsilon_{s,max}$	Damage Region
Model-1	SW-1	−0.0283	0.040	Collapse
	SW-2	−0.0278	0.040	Collapse
	SW-3	−0.0025	0.013	Significant Damage
	SW-4	−0.0026	0.012	Significant Damage
Model-2	SW-1	−0.1155	0.031	Collapse
	SW-2	−0.1157	0.031	Collapse
	SW-3	−0.0024	0.009	Significant Damage
	SW-4	−0.0024	0.009	Significant Damage
Model-3	SW-1	−0.0016	0.022	Significant Damage
	SW-2	−0.0027	0.023	Significant Damage
	SW-3	−0.0013	0.023	Significant Damage
	SW-4	−0.0027	0.010	Significant Damage

The analyses conducted under the Pazarcık (Kahramanmaraş) earthquake indicate that Model-3 remains within the Controlled Damage (CD) performance level, whereas Model-1 and Model-2 do not meet the Collapse Prevention (CP) performance level. Model-2 exhibits the most severe structural response, with nearly all first-story columns and two out of four shear walls exceeding the CP limit.

The displacement-time graphs obtained at the top floor of the models for Case-2 are presented in Figure 9. The high displacement demand in Model-1, along with the progressive increase in displacement observed in Model-2, has been identified as a key factor contributing to the failure of these models to meet the CP performance level. In contrast, Model-3 demonstrates the best seismic performance by maintaining controlled displacements and structural stability.

Figure 10 shows the total base shear resisted by the RC walls under Case-2. Model-3 experiences a relatively higher base shear demand, which highlights its capacity to withstand lateral seismic loads. In contrast, Model-1 and Model-2 exhibit a declining base shear response over time, indicating damage accumulation. The degradation in shear resistance reflects a reduced capacity to resist lateral loads, consistent with the damage identified in the analyses.

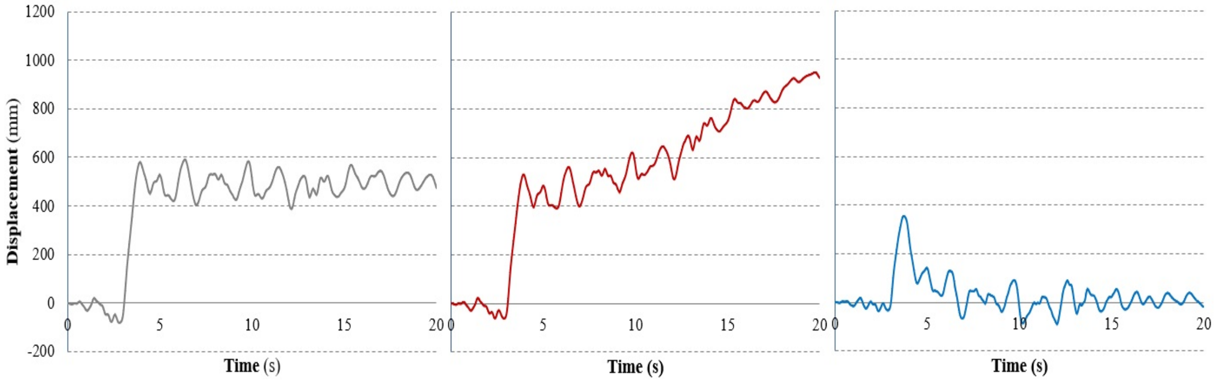

(a) (b) (c)

Figure 9. Time history of displacement at the top floor under Case-2 **(a)** Model-1 **(b)** Model-2 **(c)** Model-3

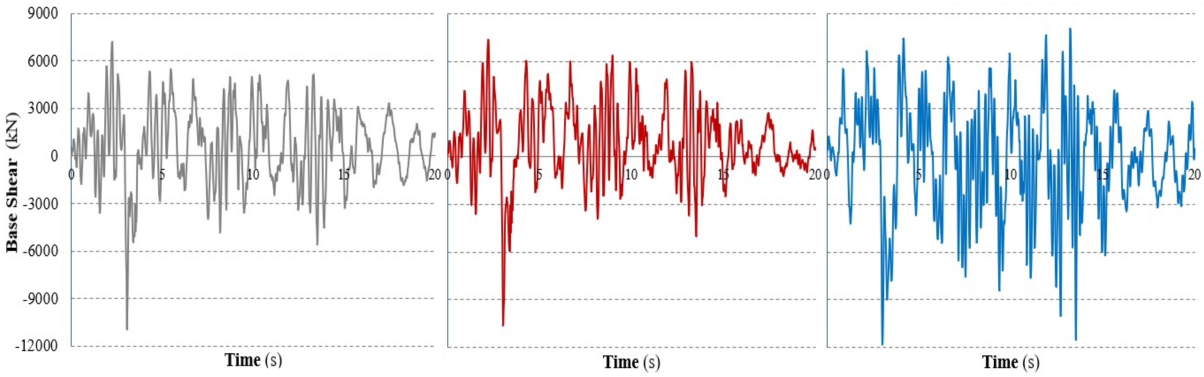

(a) (b) (c)

Figure 10. Total base shear resisted by the shear walls under Case-2 **(a)** Model-1 **(b)** Model-2 **(c)** Model-3

V. CONCLUSIONS

This study investigates the influence of shear wall layout on the seismic performance of a 10-story RC building. For this purpose, three structural models are designed in accordance with the Turkish Building Earthquake Code (TBEC-2018): Model-1 with perimeter shear walls, Model-2 with shear walls along the middle axes and Model-3 with a core shear wall. Nonlinear time-history analyses are conducted on these models using two approaches: (i) spectrally matched ground motion records (Case-1) and (ii) the ground motion record from the Pazarcık (Kahramanmaraş) earthquake (Case-2). The findings of the study are summarized as follows:

- All models satisfy the Controlled Damage (CD) performance level under Case-1, indicating that the selected shear wall layouts provide sufficient seismic resistance to design-level ground motions.
- Under Case-2, Model-3 remains within the Controlled Damage (CD) performance level, whereas Model-1 and Model-2 fail to meet the Collapse Prevention (CP) performance level. Model-2 exhibits the most severe structural response, with widespread exceedance of CP limits in vertical elements, potentially leading to structural collapse.
- Model-3 exhibits the highest base shear demand and hysteretic energy dissipation among the three models, contributing to its better seismic performance. However, special attention should be given to the

shear capacity of RC walls during the design stage, particularly in systems expected to experience significant base shear demand under strong seismic excitations.

- The displacement-time history reveals that the relatively high displacement demand in Model-1 and the progressive increase observed in Model-2 lead to the exceedance of the Collapse Prevention (CP) performance level. In contrast, Model-3 maintains a stable displacement response throughout the seismic excitation.

These findings underscore the critical influence of shear wall layout on the seismic performance of RC buildings. While all examined models satisfy the performance target under design-level ground motions, only the core shear wall layout (Model-3) provides sufficient resistance under the Pazarcık (Kahramanmaraş) earthquake, effectively preventing collapse and maintaining structural integrity.

REFERENCES

1. Darılmaz K (2012) Depreme dayanıklı betonarme binaların tasarımına giriş (in Turkish). Sage Yayıncılık, Ankara.
2. Anshuman S, Bhunia D, Ramjiyani B (2011) Solution of shear wall location in multi-storey building. International Journal of Civil and Structural Engineering 2(2):493–506.
3. Magendra T, Titiksh A, Qureshi AA (2016) Optimum positioning of shear walls in multistorey-buildings. International Journal of Trend in Research and Development 3(3):666–671.
4. Tarigan J, Manggala J, Sitorus T (2018) The effect of shear wall location in resisting earthquake. IOP Conf Ser: Mater Sci Eng 309:012077. https://doi.org/10.1088/1757-899X/309/1/012077
5. Nayel IH, Abdulridha SQ, Kadhum ZM (2018) The effect of shear wall locations in RC multistorey building with floating column subjected to seismic load. International Journal of Civil Engineering and Technology 9(7):642–651.
6. Çöğürcü MT, Uzun M (2020) Effect of configuration of shear walls at story plan to seismic behavior of high-rise reinforced concrete buildings. Challenge Journal of Structural Mechanics 6(1):31–40. https://doi.org/10.20528/cjsmec.2020.01.004
7. Mentari S, Nursani R (2021) Analysis of effective location of shear wall for high rise building with U-configuration. Jurnal Teknik Sipil & Perencanaan 23(2):167–176. https://doi.org/10.15294/jtsp.v23i2.32009
8. Bin Zahid CZ et al (2023) Different orientations of shear wall in a reinforced concrete structure to control drift and deflection. J Phys Conf Ser 2521:012006. https://doi.org/10.1088/1742-6596/2521/1/012006
9. More MR, Bhumare AS, Nagargoje SB (2023) The impact of different shear wall structure position on symmetric and unsymmetric tall buildings. International Journal for Research in Applied Science & Engineering Technology 11(IV):1218–1228. https://doi.org/10.22214/ijraset.2023.50308
10. Islam M, Mofiz SA (2024) Effect of positioning of shear walls in a multi-storied building on response to earthquake. Eng Res Express 6:025107. https://doi.org/10.1088/2631-8695/ad43b8
11. Rana S et al (2024) Investigation of reinforced concrete structure with shear walls positioned at various locations in a multi-storied residential building. Journal of Civil and Construction Engineering 10(1):42–55.
12. Lam TQK (2024) The influence of the layout of shear walls on internal forces and horizontal displacements in an 18-story building. Edelweiss Applied Science and Technology 8(3):259–278. https://doi.org/10.55214/25768484.v8i3.963
13. Ayar AZ, Fizan AA (2024) Seismic response history analysis of RC frame building with different position of shear walls by using ETABS. Journal of Mechanical, Civil and Industrial Engineering 5(2):1–9. https://doi.org/10.32996/jmcie.2024.5.2.1
14. Aminnia M, Hosseini M (2015) The effects of placement and cross-section shape of shear walls in multi-story RC buildings with plan irregularity on their seismic behavior by using nonlinear time history analyses. International Journal of Civil and Environmental Engineering 9(10):1319–1326.
15. Resatoglu R, Jkhsi S (2022) Evaluation of ductility of reinforced concrete structures with shear walls having different thicknesses and different positions. IIUM Engineering Journal, 23(2):32–44. https://doi.org/10.31436/iiumej.v23i2.2070
16. Khelaifia A, Chebili R, Zine A (2024) Impact of the position and quantity of shear walls in buildings on the seismic performance. Asian J Civ Eng 25:953–964. https://doi.org/10.1007/s42107-023-00824-w

17. Labibzadeh M et al (2024) Effect of arrangement of shear walls on the fragility curves of RC frames subjected to sequential earthquake excitations. Iran J Sci Technol Trans Civ Eng 48:2145–2175. https://doi.org/10.1007/s40996-023-01265-w
18. Sesli H, Cosgun SI, Husem M, Demir S (2016) Behavior of the reinforced concrete coupled wall systems and wall boundary elements. 12th International Congress on Advances in Civil Engineering, Istanbul, Türkiye, Sept. 21–23.
19. Sesli H, Cosgun SI, Husem M (2016) A numerical investigation of cyclic behavior of coupled wall systems. 2nd International Conference on Engineering and Natural Science, Sarajevo, Bosnia and Herzegovina, May 24–28.
20. Turkish Building Earthquake Code (TBEC, 2018), Disaster and Emergency Management Presidency, Ankara, Türkiye.
21. Disaster and Emergency Management Presidency (AFAD). https://en.afad.gov.tr/. Accessed June 2025
22. SAP2000 v23 Structural Analysis and Design Software, Computers and Structures, Berkeley, California.
23. Ibarra LF, Medina RA, Krawinkler H (2005) Hysteretic models that incorporate strength and stiffness deterioration. Earthq Eng Struct Dyn 34(12):1489–1511. https://doi.org/10.1002/eqe.495
24. Loo YC, Guan H (1997) Cracking and punching shear failure analysis of RC flat plates. J Struct Eng 123(10):1321–1330. https://doi.org/10.1061/(ASCE)0733-9445(1997)123:10(1321)
25. Miao ZW, Lu XZ, Jiang JJ, Ye LP (2006) Nonlinear FE model for RC shear walls based on multi-layer shell element and micro-plane constitutive model. In: Computational Methods in Engineering & Science. Springer, Berlin, Heidelberg, pp 204. https://doi.org/10.1007/978-3-540-48260-4_50
26. Taucer F, Spacone E, Filippou FC (1991) A fiber beam-column element for seismic response analysis of reinforced concrete structures. Report No. UCB/EERC-91/17, University of California, Berkeley.
27. Guan H, Loo YC (1997) Flexural and shear failure analysis of reinforced concrete slabs and flat plates. Adv Struct Eng 1(1):71–85. https://doi.org/10.1177/136943329700100108
28. Mander JB, Priestley MJN, Park R (1988) Observed stress-strain behavior of confined concrete. J Struct Eng 114(8):1827-1849. https://doi.org/10.1061/(ASCE)0733-9445(1988)114:8(1827)
29. Eurocode 8 (2004) Design of Structures for Earthquake Resistance - Part 1: General Rules, Seismic Actions and Rules for Building, European Committee for Standardization, Brussels.
30. Somerville PG, Smith NF, Graves RW, Abrahamson NA (1997) Modification of empirical strong ground motion attenuation relations to include the amplitude and duration effects of rupture directivity. Seismol Res Lett 68(1):199–222. https://doi.org/10.1785/gssrl.68.1.199
31. Pacific Earthquake Engineering Research Center (PEER). PEER Ground Motion Database. http://peer.berkeley.edu/smcat/. Accessed July 2025.
32. Turkish Accelerometric Database and Analysis System (TADAS). https://tadas.afad.gov.tr/. Accessed March 2025
33. Seckin A, Doran B (2023) Investigation of shear safety in reinforced concrete walls according to TBEC-2018. Turk J Civ Eng 34(5):107–128. https://doi.org/10.18400/tjce.1235472
34. Priestley MJN (2003) Does capacity design do the job? An examination of higher mode effects in cantilever walls. Bull N Z Soc Earth Eng 36(4):276–292. https://doi.org/10.5459/bnzsee.36.4.276-292